Double rotor for solid-state NMR

A. Samoson[a] and A. Pines

Materials and Chemical Sciences Division, Lawrence Berkeley Laboratory, 1 Cyclotron Road, Berkeley, California 94720 and Chemistry Department, University of California, Berkeley, California 94720

(Received 26 May 1989; accepted for publication 5 July 1989)

An NMR double-rotation probe providing for reorientation of a sample around two axes is described, and the key design features for low-friction motion are discussed. By means of double rotation, second-order broadening is averaged away, thus enhancing the resolution of spectra for quadrupole nuclei in solid-state NMR.

INTRODUCTION

Nuclear magnetic resonance (NMR) is used widely in the study of solid materials. NMR line shifts provide information about chemical bonding and short-range order around nuclear spins. Frequently, however, the experiments suffer from line-broadening effects that lower the resolution and thus make the data less sensitive to structural effects in the solid.

Spectral line shifts generally depend on the orientation of crystallites with respect to the direction of the magnetic field. In the case of a powder or polycrystalline sample, where there are many randomly oriented crystallites, individual line shifts sum to produce an inhomogeneous line broadening. This line broadening disappears if the isotropy of space, initially truncated by the unique direction of the magnetic field, is restored.

To a first approximation the isotropy of space is recovered if the magnetic field is directed along three orthogonal directions during evolution of the signal. Technically, this can be accomplished by means of "magic angle spinning" (MAS).[1] In MAS the sample powder is contained in a small axially symmetric rotor spun rapidly about an axis tilted at angle $\theta^{(2)} = 54.74°$ from the direction of the magnetic field. The cosine of the angle $\theta^{(2)}$ (the "magic angle") is a root of the second-order Legendre polynomial

$$P_2(\cos\theta^{(2)}) = 0. \tag{1}$$

The particular function $P_2(\cos\theta)$ arises from the orientational dependence of the principal interactions contributing to the line broadening in high-field NMR spectra: chemical shift anisotropy, and dipolar and first-order quadrupolar interactions. The magic angle is the angle between the edge and diagonal of a cube, cubic symmetry being the lowest-order solution for trajectories in space which exploit polyhedral symmetry for the averaging of tensor interactions.

It is well known, however, that not all line-broadening mechanisms are eliminated by a conical MAS trajectory of directions of the magnetic field (the extension of three orthogonal directions to a continuum). A common example is the case of second-order quadrupolar broadening where MAS provides only a fourfold reduction in linewidth.[2] The next approximation to an isotropic distribution of magnetic field directions is a continuous trajectory induced by two superimposed conical motions. It has been pointed out[3] that effective resolution enhancement for second-order effects can be achieved if the apex angles $2\theta^{(2)}$ and $2\theta^{(4)}$ of the cones are determined by Eq. (1) together with

$$P_4(\cos\theta^{(4)}) = 0, \tag{2}$$

and if the ratio of (nonzero) frequencies of the inner (ω_i) and outer (ω_o) rotors satisfies

$$\frac{\omega_i}{\omega_o} \neq n \text{ or } \frac{1}{n} \text{ when } n = 1, \frac{4}{3}, \frac{3}{2}, 2, 3, 4. \tag{3}$$

Particularly efficient is any ratio $\omega_i/\omega_o \geqslant 5$. Note that in contrast to Eq. (1), Eq. (2) has two solutions: $\theta_1^{(4)} = 30.6°$ and $\theta_2^{(4)} = 70.1°$.

In the laboratory frame the desired multiple spinning can be achieved by two rotors, one embedded in the other (Fig. 1). The axis of the inner rotor is inclined by θ_i with respect to the axis of the outer rotor. The spinning axis of the outer rotor forms an angle θ_o with the direction of the magnetic field, where either

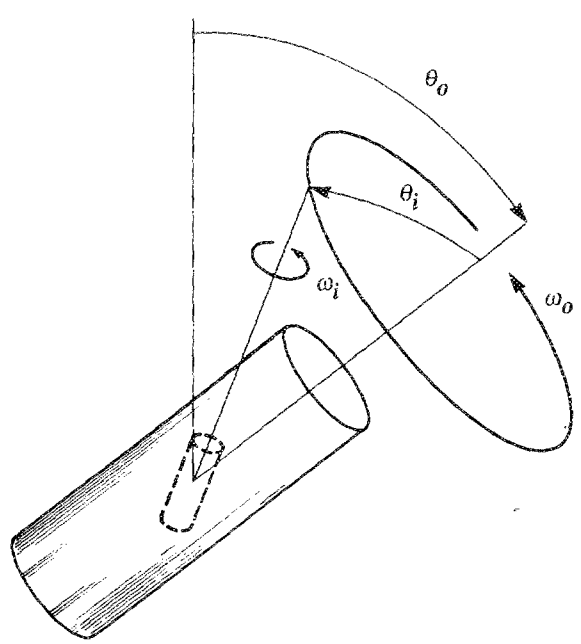

FIG. 1. Double-rotor configuration. Definition of motions and angles.

 0034-6748/89/103239-03$01.30

$$\theta_i = \theta^{(2)};\ \theta_o = \theta^{(4)} \tag{4}$$

or

$$\theta_i = \theta^{(4)};\ \theta_o = \theta^{(2)}. \tag{5}$$

The polyhedral symmetry relevant to the averaging of second-order broadening is that of an icosahedron.[4]

I. DOUBLE ROTOR

Consider the double-rotor configuration of Fig. 1. As the angular frequency of the outer rotor approaches 1 kHz, the inner rotor acts as a small gyroscope and exerts a torque upon its housing. Depending on the type of bearing employed, the torque may not only increase resistance to the motion, but prohibit it completely. Rather than optimize the load capacity of the bearings, we have opted for reduction of the torque. It is well known that for motions such as those implemented by a double rotor, the torque can be eliminated if the frequencies of internal and external spinning satisfy[5]

$$\omega_i = \cos(\theta_i)\,\frac{I_{\rm tr} - I_{\rm ax}}{I_{\rm ax}}\,\omega_o, \tag{6}$$

where $I_{\rm tr}$ and $I_{\rm ax}$ are the transverse and axial moments of inertia of the inner rotor. For a homogeneous cylindrical body of mass M, diameter d, and length l, these moments are readily evaluated:

$$I_{\rm ax} = \frac{Md^2}{8}, \tag{7}$$

$$I_{\rm tr} = M\left(\frac{d^2}{16} + \frac{l^2}{12}\right). \tag{8}$$

Assuming that the frequency ratio of the two rotors is 5, $\omega_i = 5\omega_o$, Eqs. (4)–(7) allow an estimation of the geometrical factors relevant to the NMR sensitivity. The values in the Table I are calculated for the case of a solenoidal pickup coil coaxial with the outer rotor. The length and diameter of the coil are chosen to accommodate the (tilted) inner rotor, and the NMR sensitivity is $\sin\theta_o \times$filling factor. The design with maximum sensitivity was realized experimentally as in Fig. 2. The diameter of the inner rotor (1) is 5 mm, the ratio of length to the diameter is 3.08, according to the Eq. (6), and the internal tilt angle $\theta_i = 30.6°$. For maximum speed, both rotors (1 and 2) are suspended on air bearings[6] (3 and 4, respectively) and driven by air jets (5 and 6). The bearings are close to the ends of the rotors in order to withstand loads caused by possibly unbalanced moments. The air bearing configuration is comprised of orifices forming streams of pressurized air which impinge upon impeller grooves. The surface of the outer rotor has two rings of grooves next to the bearing surface, while the inner rotor has one ring of grooves in the middle. A critical feature of the system is the maintenance of air compression in the channels of the moving rotor. The outer rotor has inlets on each end that enable pressurized air to enter and feed the bearing and drive of the inner rotor via machined channels. The inlets, in the form of cylindrical passages in the outer rotor, surround hollow immobile protrusions (7 and 8) with very small clearance. The drop of air pressure between the protrusion and the passage does not exceed 50%. The air pressure in each of the four air channels (7–10) is controlled independently.

Due to the asymmetry of the air channels and the tilted assembly of the inner rotor, translational as well as conical whirl modes of motion of the outer rotor may arise. Both the

TABLE I. Geometric factors for various configurations of the double rotor.

θ_i	θ_o	Filling factor	NMR sensitivity
30.6	54.7	0.165	0.135
54.7	30.6	0.097	0.049
54.7	70.1	0.097	0.091
70.1	54.7	0.080	0.065

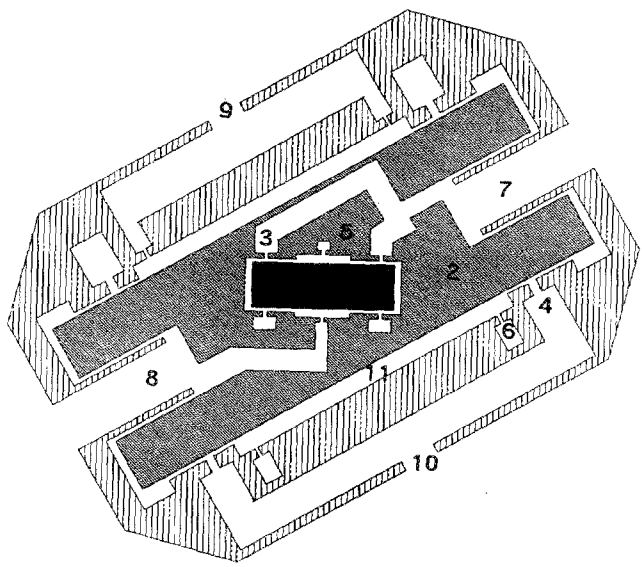

FIG. 2. Routing of compressed air to bearings and drives: (1) inner rotor (dark area), (2) outer rotor, (3,4) air bearings, (5,6) drives, (7,8) passage of compressed air to housing of inner rotor, (9,10) inlets of compressed air for drive and bearing of outer rotor, and (11) space for detection coil.

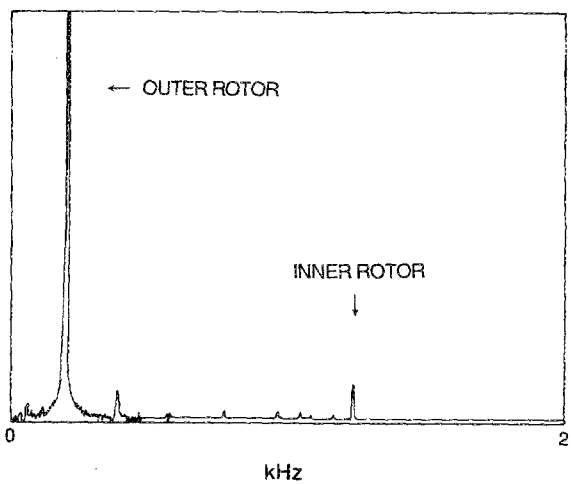

FIG. 3. Piezofilm vibration spectrum of the double rotor during start up. The most intensive peak corresponds to the motion of the outer rotor at 200 Hz. Clearly visible is the first harmonic due to conical whirl mode of this motion. The inner rotor's frequency of 1200 Hz is evidenced by the third peak.

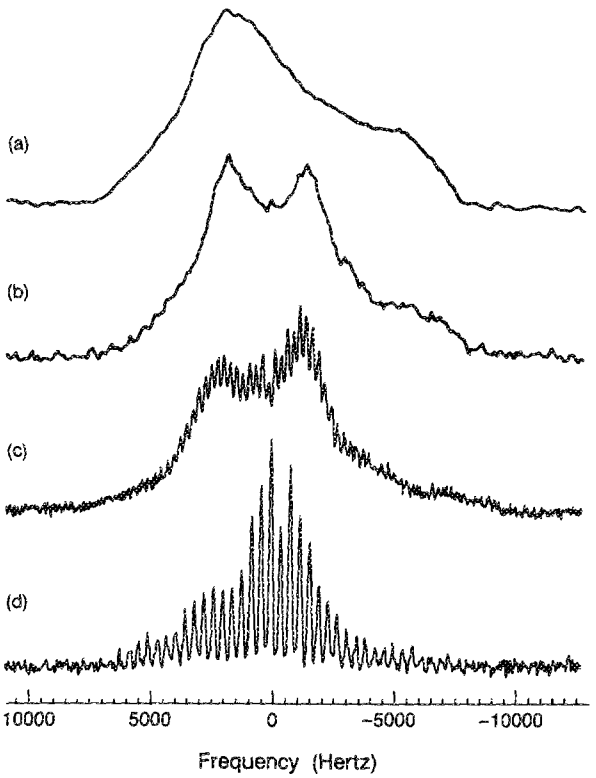

FIG. 4. Enhancement of resolution for the central transition of ^{23}Na in sodium oxalate. Spectra of (a) static and (b)–(d) doubly rotating samples are shown. The frequency of the outer rotor is (b) 150 Hz, (c) 250 Hz, and (d) 400 Hz, while the inner rotor frequency increases from 1 to 3 kHz.

unbalanced force and moment can be corrected by the addition or removal of balance weights in two separate planes along the length of the rigid rotor.[7] The outer rotor has hollow cavities on both ends for the purpose of fine tuning the balance. The outer rotor was machined from VESPEL,[8] the inner from DELRIN.[9]

Operation of the double-rotor system begins with the activation of the inner rotor and subsequent increase in the speed of both rotors. The startup of the system can be monitored in real time by inspecting the spectrum of vibrations of the double-rotor assembly. A piezofilm mounted on the housing of the outer rotor provides voltage oscillations which are Fourier analyzed and accumulated in magnitude mode. Some tens of accumulations are sufficient to extract the rotation frequencies of both the outer and inner rotors; an example is shown in Fig. 3.

The effect of double rotation was checked on the NMR spectrum of sodium-23 in solid sodium oxalate at 106 MHz. The second-order quadrupolar line broadening of 13 kHz determines the shape of central transition in a static sample [Fig. 4(a)]. At low speeds, the linewidth (but not the shape) is still comparable to that of the static spectrum [Fig. 4(b)]. With an increase in speed, the period of rotation becomes shorter than the decay time of the signal, rotational echoes emerge, and Fourier transformation yields a line shape modulated at the frequency of the outer rotor [Fig. 4(c)]. Eventually, the spectrum consists of a resolved spinning center band and spinning sidebands [Fig. 4(d)]. The spinning sidebands are readily identified since they shift with the frequency of the outer rotor. The ultimate resolution is determined by residual linewidth due to fourth-order effects and homonuclear dipolar couplings.

Recent developments have dealt with DOR sideband suppression[10] and with the application of DOR to oxygen-17 NMR in solids.[11]

ACKNOWLEDGMENTS

We are grateful to G. C. Chingas for helpful discussions and for assistance in technical matters. This work was supported by the Director, Office of Energy Research, Office of Basic Energy Sciences, Materials Sciences Division of the U. S. Department of Energy under Contract No. DE-AC03-76SF00098.

[a] Permanent address: Institute of Chemical Physics and Biophysics, Tallinn, Estonia.

[1] E. R. Andrew, A. Bradbury, and R. G. Eades, Arch. Sci. **11**, 223 (1958); I. J. Lowe, Phys. Rev. Lett. **2**, 285 (1959); S. F. Dec, R. A. Wind, and G. E. Maciel, J. Magn. Reson. **70**, 355 (1986).
[2] A. Samoson and E. Kundla, Abstracts of the 5th Specialized Colloque AMPERE, Uppsala, 1981, p. 37.
[3] A. Samoson, E. Lippmaa, and A. Pines, Mol. Phys. **65**, 1013 (1988); A. Llor and J. Virlet, Chem. Phys. Lett. **152**, 248 (1988).
[4] A. Samoson, B.-Q. Sun, and A. Pines (unpublished).
[5] L. Landau and E. Lifshits, *Mekhanika* (Moscow) **1973**, 142 (1973).
[6] F. D. Doty and P. D. Ellis, Rev. Sci. Instrum. **52**, 1868 (1981).
[7] N. F. Rieger, Balancing of Rigid and Flexible Rotors, The Shock and Vibration Information Center, United States Department of Defense, 1986, p. 7.
[8] VESPEL is a registered trade name of E. I. Dupont DeNemours Co. for polymethylene oxide.
[9] DELRIN is a registered trade name of E. I. Dupont DeNemours Co. for polyimide resin.
[10] A. Samoson and E. Lippmaa, J. Magn. Res. (in press).
[11] B. F. Chmelka, K. T. Mueller, A. Pines, J. Stebbins, Y. Wu, and J. W. Zwanziger, Nature **339**, 42 (1989).